PHILIPPINE ENGINEERING JOURNAL
PEJ 2013; Vol. 34, No. 1: 47-65

HEAT AND MASS TRANSFER IN AN ADSORPTION PANEL WITH ROD FINS HEATED BY A RADIANT SOURCE: 3D MATHEMATICAL MODEL

Rizalinda L. de Leon[1], Arturo B. Cortes[2], Richard Q. Chu[1]
[1]Department of Chemical Engineering,
College of Engineering, University of the Philippines, Diliman, Quezon City
[2]Department of Mining, Metallurgical and Materials Engineering
College of Engineering, University of the Philippines, Diliman, Quezon City

ABSTRACT

A 3-D modified equilibrium, static-bed model of adsorption in an adsorption panel with rod fins heated by a radiant heat source is developed and solved using the Method of Lines. The energy equation is transformed to have only one dependent variable hence the accumulation, conduction and generation terms are all expressed in terms of rate of change and gradient of the local bed temperature. Results are compared with experimental data for insight into the heat and mass transfer process occurring in the bed during the cooling and heating phases. Effective surface diffusivities derived agree with literature values obtained by other authors.

Keywords: *diffusivity, effective thermal conductivity, method of lines*

1. INTRODUCTION

Adsorption or physical adsorption is a process wherein gas or liquid molecules attach to solid surfaces by van der Waals and electrostatic forces. Adsorption systems can be classified as either dynamic or static. Dynamic adsorption involves fluid flowing through the fixed or fluidized adsorbent bed. The fluid is usually some inert gas that may or may not contain the adsorbate, depending on the operation required. Dynamic beds are characterized by relatively high heat and mass transfer rates that are strongly dependent on fluid velocities. On the other hand, static adsorption occurs in closed systems that are characterized by relatively lower heat and mass transfer rates since the adsorbate does not flow through the bed, but rather disperses into the bed by diffusion or low-velocity convection.

Dynamic adsorption has found application in a number of separation processes, such as in the separation of nitrogen and oxygen from air using molecular sieves, waste treatment and purification processes. Static adsorption, on the other hand, is used in refrigeration and heat pump applications. The advantages of adsorption-type refrigerators and heat pumps over the conventional refrigeration systems are that they do not require compressors, are driven by relatively low-temperature heat sources such as solar energy or waste heat, and they have no moving parts.

*Corresponding author: Telefax: +632 929 6640, e-mail address: rldeleon@up.edu.ph (R.L. de Leon)

Received: June 28, 2012
Accepted: November 5, 2012

Studies on heat and mass transfer in static adsorption beds used for cooling applications have been done by a number of researchers. Suzuki and Kawazoe (1974 and 1975) and Suzuki and Chihara (1982) did parametric studies to show how the rate of adsorption changes depending on which mass transfer mechanism is controlling. Their results are collectively discussed by Suzuki (1989). Sun, et al (1986) calculated the temperature and concentration distributions inside a spherical grain of adsorbent when subjected to a step-change in pressure of adsorbable vapor. Kaviany (1991) present a chronological tabulation of contributions to transport in porous media starting from the 1800s to 1991. Pons (1998) investigated the phenomenon of adsorbate redistribution in beds with large temperature variations during pressure changes and found that the redistribution tends to minimize the temperatrure differences within the bed, but that it had no effect on the performance of the system.

The idea of an effective thermal conductivity was first put forward by Maxwell in 1873 as cited by Batchelor and O'Brien (1977). The determination of the effective thermal conductivity of adsorbent beds has been carried out by Kunii and Smith (1960), who suggested a correlation between with bed void fraction and the solid-to-fluid thermal conductivity ratio. Aittomaki and Aula (1991) likewise used transient temperature profiles to measure effectivity of an adsorption bed. Gurgel (1998) measured the thermal conductivity of silica gel at different pressures and water content.

The effective or apparent mass diffusivity of water in silica gel and NaX zeolite pellets were determined by Chihara and Suzuki (1983), Gurgel, et al (2001), Qin and Baoqui (2001) and Ni and San (2002). Their experiments showed that pressure and concentration have very small effects on the effective diffusivity, and that the diffusivity may be expressed as a function of temperature according to an Arrhenius-type equation. Various mechanisms of mass transfer may be occurring either sequentially or in parallel fashion in a static adsorption bed. Each mechanism may be characterized by their respective diffusion coefficients and may include diffusion through a stagnant film around the adsorption pellet (D_m), gas diffusion through the pores (D_m), Knudsen diffusion (D_K), and surface diffusion within the solid pore walls (D_s).

Ni and San (2002) measured the apparent solid-side mass diffusivity of water in regular density silica gel (particle density = 1270 kg/m^3, pore size = 2nm, particle diameter = 2 mm) over a range of temperatures, and found that the D_{app} ranges from 2 x 10^{-9} m^2/s at 79.6 ^{o}C, to 2.5 x 10^{-11}m^2/s at 5.1 ^{o}C. These values were measured at atmospheric pressure in the presence of air. Under vacuum conditions and in the absence of air, molecular diffusion is no longer the dominant mechanism for pore diffusion. Using an Arrhenius type equation with experimentally evaluated pre-exponential coefficient and activation energy for surface migration, an order of magnitude of 10^{-5} m^2/sec could be calculated for the Knudsen diffusivity, in the pore size mentioned.

Chihara and Suzuki (1983) considered the case wherein surface diffusion of water in silica gel is rate-determining and obtained a pre-exponential factor and activation energy of surface diffusion. These are used to estimate the order of magnitude of the surface diffusivity to be 1 x 10^{-11} m^2/sec at 298 K. Given the above order of magnitude estimates of the different mechanisms, and if the mechanisms of pore diffusion and surface diffusion are assumed parallel (Suzuki, 1989), the contribution of surface diffusion is small compared to that of pore diffusion. But if the mechanisms of surface diffusion were in series with that of pore diffusion, then surface diffusion will be controlling and will have a significant effect on the heat and mass transfer in the adsorption bed.

Different mathematical models of static adsorption beds have been put forward, solved and compared with experimental measurements. Sakoda and Suzuki (1986) used a uniform-temperature and uniform-concentration model which included a heat balance, a linear driving force mass transfer equation and an equation of state for the adsorption pair. The packed bed they used had rectangular plate fins to enhance heat transfer. Results of their calculations had good agreement with experimental data. Guilleminot, et al (1987) analyzed the heat transfer inside a finned, false bottom adsorption bed using a uniform pressure, non-uniform temperature model assuming negligible resistance to mass transfer. The model was found to be highly sufficient for solar-heated adsorbers where heat transfer is the rate-limiting factor. Passos, et al (1989) also used a uniform pressure model, but accounted for mass transfer resistances within the pellets. Good agreement with experiment measurements was also noted in this case.

Hajji and Khalloufi (1995) validated the constant pressure model of heat and mass transfer derived from local thermodynamic equilibrium. Their work showed that the thickness of the adsorbent bed as well as the heat transfer coefficient between adsorbent and the heating or cooling medium significantly affect adsorption rates and cooling capacity. In 1996 the same researchers reported in improving heat exchange performance of adsorbers using a finned-bed structure. Fedorov and Viskanta (1999) investigated the interactions between heat and mass transfer during dynamic adsorption/desorption in a honeycomb structure. Marletta et al (2002) presented a two-dimensional heat and mass transfer model for a non-uniform pressure, non-uniform temperature case case. Leong and Liu (2004) described the transient two-dimensional heat and mass transfer in a zeolite NaX/water system. They accounted for internal and external mass transfer limitations. Various other researchers such as Cortes et al (2009), Hassan et al (2011) applied earlier models to predict the performance of solar-heated activated coal or charcoal-methanol systems in cylindrical coordinates. Zhang, et al (2011) used a lumped parameter model for studying the effect of operating conditions on a solar-heated silica gel-water adsorption chiller.

The models used in the above studies can be classified into two types: a heat transfer model, which neglects the effects of mass transfer on the resulting temperature profile, and a heat and mass transfer model which accounts for diffusion and convection in either the gas or solid phases or both. Yong and Sumathy (2004) compared a heat transfer model with a heat and mass transfer model to lay down criteria for the validity of a purely heat transfer model. Their study showed that the heat transfer model is valid for adsorption systems with low heat flux such as solar-heated adsorbers.

The second order parabolic partial differential equations (PDEs) which describe heat transfer in adsorption beds during adsorption and desorption have been solved using a number of different methods. A summary of methods used for the solution of transient heat equation without a generation term has been discussed by Patankar (1980). For a one-dimensional system, the explicit Euler and the implicit Crank-Nicolson (CN) methods have often been used and compared. A tri-diagonal matrix algorithm is used to solve the CN system of equations. For two- to three-dimensional systems, the resulting system of equations no longer result in a tridiagonal matrix. Instead, an iterative method such as the Gauss-Seidel or the Successive Over-Relaxation (SOR) methods are recommended. Another method that can be used is the Alternating Direction Implicit (ADI) method originally developed by Peacemean and Rachford (1955) for two-dimensional equations and extended for three-dimensional problems by Douglas and Gunn (1964).

Some of the methods used specifically to solve heat and mass transfer adsorption models include a discretizing the set of second order PDEs using a forward difference scheme (FDS) for the time derivative and boundary conditions, the quickest upstream difference shceme (QUDS) for the spatial derivatives and the central difference scheme (CDS) for the second order spatial derivatives (Marletta, 2002). Leon and Liu (2004) discretized the convection terms using a power law scheme, and similarly used CDS and FDS for the diffusion/convection derivatives and time derivative, respectively. To solve the resulting implicit systems of equations, they used the line-by-line method which is a combination of the tridiagonal matrix algorithm (TEMA) and the Gauss-Seidel iteration procedure.

Scheisser (1991) proposed the Method of Lines, where only the spatial derivatives of the PDE are discretized. This results in a system of ordinary differential equations (ODEs) which can be solved using either an Euler or a Runge-Kutta procedure. The method has been used in the solution of optics problems in physics (Kremer, 1994; Yang and Pregla, 1995) and in the solution of unsteady state heat transfer (Cutlip, 1998).

This paper reports the use of a modified 3-D heat conduction equilibrium model of a silica gel-water adsorption bed heated by a constant radiant heat source. The modification consists of the application of a correction factor on the heat conduction term to account for convective transport, and a correction factor on the heat generation term to account for limiting mass transfer. Using the Method of Lines, transient bed temperature profiles during heating and cooling were generated. The model is fitted to experimental profiles to evaluate observed effective thermal conductivity and mass diffusivity.

Experimental temperature profiles were obtained from a 25.4-cm diameter, 5 cm deep adsorption bed connected to a reservoir described in another paper. Fifty-two rod fins, 7 mm in diameter, are screwed into the top plate and run the depth of the packed bed down to the bottom plate. Details of the adsorption system are described in another paper.

2. THE MATHEMATICAL MODEL

A 3-D mathematical model for heat transfer through the adsorption bed with rod fins was developed and used to generate temperature profiles and temperature progressions that were compared with the experimental data collected. The mathematical model, discussed in more detail in another paper, consisted of a modified 3-dimensional equilibrium transient heat conduction equation with heat generation (Equation 1).

$$\frac{\partial(\rho_b C_b T)}{\partial t} = k_b \nabla^2 T + q_v \tag{1}$$

In the equation, k_b is the effective bed thermal conductivity. In a static bed, the effective bed thermal conductivity may be estimated using the Kunii-Smith correlation (Kunii and Smith, 1960) based on the bed void fraction ε, a contribution of solid-to-solid heat transfer through a thin layer of fluid around a contact point of adjacent particles φ, and the thermal conductivities of the solid particles k_s and of the vapor occupying the voids k_f. The correlation is given for the static bed effective thermal conductivity k_{eo} by Equation 2.

$$(2)\quad \frac{k_{eo}}{k_f} = \varepsilon + \frac{(1-\varepsilon)}{\varphi + \frac{2}{3}\left(\frac{k_f}{k_s}\right)}$$

The term q_v in Equation 1 is the heat generated per unit volume if heat and mass transfer rates were rapid enough to ensure that the solids are in equilibrium with the vapor at any time during adsorption or desorption (Equation 3).

$$(3)\quad q_v = \rho_b \Delta H_{ads} \frac{\partial w'}{\partial t}$$

The variable w' is the uptake or the amount of adsorbed phase per unit amount of adsorbent at any time. ΔH_{ads} is the isosteric heat of adsorption which can be expressed in terms of local temperature T and the evaporator or condenser temperature T_1 via the adsorption potential A and the Antoine equation.

The rate of uptake $\partial w'/\partial t$ depends upon the instantaneous uptake and the controlling mass transfer mechanism. If the rate of uptake were fast enough such that equilibrium uptake w may be assumed, then the uptake w' may be replaced by the equilibrium uptake w. (Equation 4)

$$(4)\quad q_{veq} = \rho_b \Delta H_{ads} \frac{\partial w}{\partial t}$$

A transformed Dubinin-Astakhov equilibrium relation was used to describe the equilibrium uptake as a function of the bed temperature T (Equation 5).

$$(5)\quad w = w_{sat}\left(\exp\left[\left(\frac{M\Delta H_v}{R}\right)\left(\frac{1}{T}-\frac{1}{T_1}\right)\right]\right)^{\frac{1}{n_F}}$$

where w_{sat} is the equilibrium uptake at saturation when relative humidity is 100% and n_F is an empirical parameter to accommodate both surface and micropore adsorption known to occur in silica gel-water systems. In transforming the Dubinin-Astakhov equilibrium relation, the Clausius-Clapeyron equation was used to express the pressure ratio in terms of the local temperature T and the evaporator or condenser temperature T_1. ΔH_v is the heat of vaporization of water.

An expression for $\partial w/\partial t$ can be obtained by taking the derivative of the equilibrium uptake w with respect to the bed or local temperature T in Equation 5 and multiplying the result by the rate of change of temperature with time $\partial T/\partial$t (Equation 6).

$$(6)\quad \frac{\partial w}{\partial t} = \frac{w_{sat} M\Delta H_v}{n_f R}\left[\exp\left(\frac{M\Delta H_v}{R}\left(\frac{1}{T}-\frac{1}{T_1}\right)\right)\right]^{1/n_f}\frac{1}{T^2}\frac{\partial T}{\partial t}$$

Hence the heat generation term becomes (Equation 7).

$$(7) \quad q_v = \rho_b \Delta H_a \left[\left(\frac{w_{sat} M \Delta H_v}{n_f R} \right) \exp\left(\frac{M \Delta H_v}{R} \left(\frac{1}{T} - \frac{1}{T_1} \right) \right) \right]^{1/n_f} \frac{1}{T^2} \frac{\partial T}{\partial t}$$

Substituting into the energy equation, factoring out $\partial T/\partial t$ and applying correction factors, the modified energy equation is shown in Equation 8.

$$(8) \quad \frac{\partial (\rho_b C_b T)}{\partial t} = f_k k_{eo} \nabla^2 T + \frac{q_{veq}}{f_{qv}}$$

The modification consists of applying two factors: (1) a heat generation correction factor $f_{qv} = q_{veq}/q_v$ which is a measure of deviation from the equilibrium assumption, and; (2) an effective thermal conductivity correction factor $f_k = k_b/k_{eo}$ which accounts for thermal currents in the interparticle voids and is a measure of deviation from the static bed assumption.

The math model is transformed into a dimensionless form based on the bed depth L_x, initial temperature T_o, maximum surface temperature T_{max}, and the thermal diffusivity of the top plate α_{pt} (Equation 9).

$$(9) \quad \frac{\partial \phi}{\partial \tau} = \frac{1}{\rho C \alpha_{pt}} \left[\frac{\partial}{\partial X} k \frac{\partial \phi}{\partial X} + \frac{\partial}{\partial Y} k \frac{\partial \phi}{\partial Y} + \frac{\partial}{\partial Z} k \frac{\partial \phi}{\partial Z} \right] + Q_v$$

where ϕ is the dimensionless temperature $\phi = \dfrac{(T - T_o)}{(T_{\max} - T_o)}$, τ the dimensionless time $t\alpha_{pt}/L^2_x$ while X, Y and Z are the dimensionless position variables x/L_x, y/L_x and z/L_x, respectively. Q_v is a dimensionless heat generation term given by Equation 10.

$$(10) \quad Q_v = \frac{q_v L_x^2}{\alpha_{pt} (T_{\max} - T_o) \rho C}$$

Recall that the rate of heat generation q_v is dependent on the rate of adsorption $\partial w/\partial t$ which in turn has been expressed in terms of the rate of temperature change with time. Hence, Q_v can be written in dimensionless form as,

$$(11) \quad Q_v = Q'_v \frac{\partial \phi}{\partial \tau}$$

where Q'_v is the coefficient of the dimensionless heat generation Q_v, given by Equation (12) below.

$$(12) \quad Q'_v = \left(\frac{\Delta H_{ads} w_{sat} M \Delta H_v}{C n_f R} \right) \left[\exp\left(\frac{M \Delta H_v}{R} \left(\frac{1}{T} - \frac{1}{T_1} \right) \right) \right]^{1/n_f} \frac{1}{T^2}$$

which has a non-linear dependence on temperature.

Substituting Equation (12) into Equation (9), we obtain

$$(13)\quad \frac{\partial \phi}{\partial \tau} = \frac{\frac{1}{\rho C \alpha_{pt}}\left[\frac{\partial}{\partial X} k \frac{\partial \phi}{\partial X} + \frac{\partial}{\partial Y} k \frac{\partial \phi}{\partial Y} + \frac{\partial}{\partial Z} k \frac{\partial \phi}{\partial Z}\right]}{\left(1 - Q'_v\right)}$$

Incorporating the correction factors f_k and f_{qv}, we get

$$(14)\quad \frac{\partial \phi}{\partial \tau} = \frac{\frac{f_k}{\rho C \alpha_{pt}}\left[\frac{\partial}{\partial X} k \frac{\partial \phi}{\partial X} + \frac{\partial}{\partial Y} k \frac{\partial \phi}{\partial Y} + \frac{\partial}{\partial Z} k \frac{\partial \phi}{\partial Z}\right]}{\left(1 - Q'_v \big/ f_{qv}\right)}$$

Further simplifications may be applied, for example the bed is taken to be isotropic such that the thermal conductivity k is the same in any direction.

The effective thermal conductivity of a stagnant bed layer next to the panel wall, designated by the symbol k_w is estimated using the Kunii-Smith correlation using a void fraction applicable near the wall. Ofuchi and Kunii (1965) studied variations in the effective thermal conductivity next to the wall for packed beds of spherical particles in stagnant fluids k_{ewo}, and suggested a semi-empirical relation which assumes k_{ewo} to be uniform over a distance of half a particle diameter (d_p/2) from the wall.

2.1 Initial Conditions

For this study, the experiments were done such that heating was initiated after allowing the bed to cool down to approximately uniform temperature overnight. Overnight cooling allows the bed to adsorb the maximum amount of water vapor from the reservoir limited only by the final bed and reservoir temperatures which are in thermal equilibrium with the ambient, T_a. The cooling run, on the other hand is initiated by simply turning off the radiant heat source.

Considering the above procedure, for the numerical simulation, initial conditions vary depending on whether computations are in the cooling mode or in heating mode. For the heating mode, the initial condition is such that the bed is at uniform temperature $T_{o,des}$ and uptake w_o. On the other hand, for the cooling mode, the initial condition is $T_{o,ads}(x,y,z)$ which is also the final condition of the desorption or heating mode $T_{f,des}(x,y,z)$.

$$(15)\quad T_{o,des} = T_a \text{ for all x,y,z at time t < 0, (before heating starts)}$$

$$(16)\quad T_{o,ads}(x, y, z) = T_{f,des}(x, y, z) \text{ (at start of cooling)}$$

2.2 Boundary Conditions

Figure 1 below shows a cross-sectional view from the side of a portion of the panel with the glass cover, top plate, fins, adsorbent, bottom plate and insulation indicated. The heat effects at the top of the panel are also illustrated. A discussion of the energy balance in flat-plate solar collectors is given by Garg and Prakash (2000).

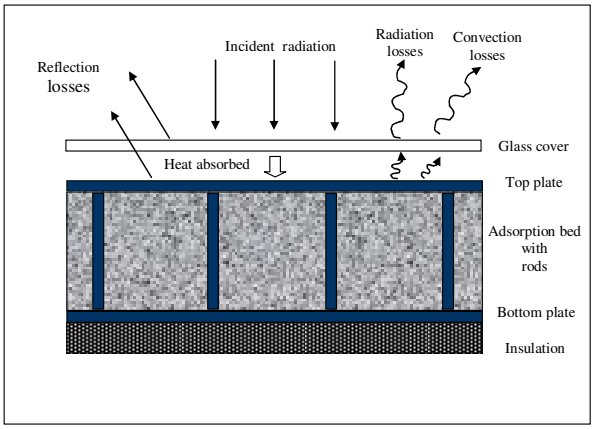

Figure 1. Heat effects at the top of a flat plate solar collector

The circular adsorption panel containing the adsorbent is bounded at the top by the outer surface of the collector plate, and at the bottom by the interface between the bottom plate and the insulation material. A square section of the bed surrounding a fin far from the panel walls is chosen as the computational domain where entrance effects may be neglected. The lateral boundaries of the square domain are defined such that the corners of the square are the midpoints of center-to-center lines between adjacent fins. Symmetry considerations further reduce the computational domain to only a quarter of the aforementioned section as shown in Figure 2 below. The insulated bottom boundary and the side boundaries of the final computational domain are described by Neumann boundary conditions $\partial T/\partial x = 0$.

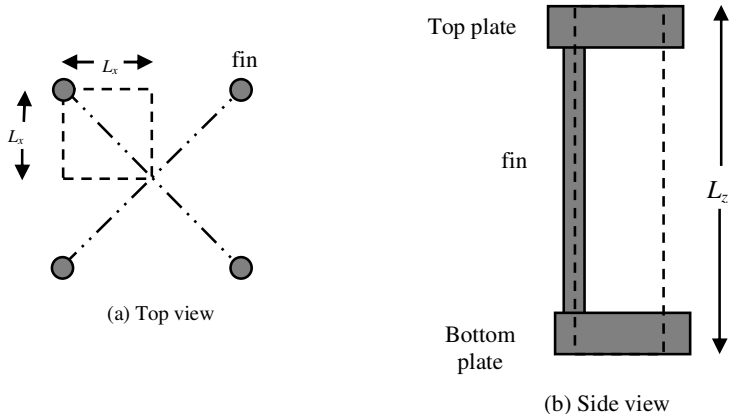

Figure 2. Boundaries and dimensions of the computational domain (a) top view and (b) side view

Useful heat Q_u is the portion of the incident radiation per unit area I_{tot} absorbed by the top plate of area A. This useful heat is eventually conducted into the bed. The energy absorbed by the top plate is given by $I_{tot}A(\tau\alpha)_e$ however, some of this is lost by radiation and convection from the top, bottom and sides. The radiative and convective losses are lumped together and characterized by an overall heat loss transfer coefficient U_L and the temperature difference between the top plate surface and ambient $(T_p - T_a)$ (Equation 17).

$$(17) \quad Q_u = A\left[I_{tot}(\tau\alpha)_e - U_L(T_p - T_a)\right]$$

As pointed out earlier the overall heat transfer coefficient U_L, is the sum of heat transfer coefficients at the top U_t, at the panel bottom U_b and at the sides or edges of the collector U_e.

$$(18) \quad U_L = U_t + U_b + U_e$$

Klein (1975) analyzed heat losses at the top of a solar flat plate collector and proposed a rigorous correlation to estimate U_t given the number of glass covers, the spacing between plates, and the emittances of the glass cover ε_g and absorber plate ε_a, and the wind heat transfer coefficient h_w. U_t is only slightly sensitive to mean plate temperatures and plate surface emissivity, but very sensitive to wind velocities. Regression analysis of results from Klein's correlation along with corrections for fitting to measured heat fluxes from the top plate were done to obtain a simpler correlation dependent only on temperature difference and wind velocity (Equation 19).

$$(19) \quad Q_u = \left(-5.18757V_{wind} - 6.70009\right)\left(T_p - T_a\right) + I_{tot}\left(\tau\alpha\right) - 2.66819V_{wind}$$

2.3 Properties and Parameters

For ease of programming and to reduce the number of program computations, average values of bed and particle properties between 298 K and 373K were used in the numerical simulation.

Particle void fraction ε_p was calculated to be 0.423 based on typical values of the particle density ρ_p and the density of pure silicon dioxide ρ_s.

$$\varepsilon_p = 1 - \frac{\rho_p}{\rho_s} = 1 - \frac{1258}{2201} = 0.423$$

The densities of the silica gel bed ρ_b and the silica gel bed adjacent to a wall ρ_w for different uptakes w were determined from experimental data. These, along with void fractions and particle density are used to estimate the effective thermal conductivities of the bed, k_{eo} and of the bed layer next to the wall k_{ewo}. The bed void fraction far from the wall was derived from the particle and bulk densities of silica gel.

$$\varepsilon_b = \frac{V_{voids}}{V_{bed}} = \frac{V_{bed} - V_{solids}}{V_{bed}} = \frac{V_{bed} - NV_p}{V_{bed}}$$
$$= 1 - \frac{NV_p}{V_{bed}} = 1 - \frac{\rho_b}{\rho_p}$$

The heat capacities of the bulk bed C_b and of the bed layer next to a wall C_w were evaluated using a mixing rule based on the mass fraction of each bed component namely, the dry silica gel (*s*), the adsorbed moisture (*a*) and the water vapor in the bed voids (*v*).

$$C = C_s X_s + C_a X_a + C_v X_v$$

The mass fraction of the vapor X_v was estimated from the total void fraction ε_T and the densities of the vapor ρ_v and the solid with adsorbed phase ρ_{s+a}. Since the mass fraction of vapor is small compared to the mass fraction of the solid and the adsorbed phase, the mass fraction of the adsorbed phase X_a was estimated from the uptake and was given by $w/(1+w)$. The mass fraction of the solid X_s was determined by difference.

Temperature-dependent thermal conductivities and heat capacities of pure silicon dioxide and steam were taken from literature (Yaws, 2009; Brodkey and Hershey, 1988). Properties of the adsorbed phase were assumed to be the same as those of saturated liquid.

At the particle void fraction of 0.423, the thermal conductivity of a silica gel particle was estimated to be 0.1527 W/m-K at 298 K. A summary of average values of derived properties is given in Table 1.

Table 1 Average properties of Amelco® silica gel and silica gel-water bed.

Property	symbol	value	units
particle density (dry basis)	ρ_p	1258.8	kg/m^3
bulk density (dry basis)	ρ_b	604.15	kg/m^3
bulk density adjacent to wall (dry basis)	ρ_w	377.64	kg/m^3
bed void fraction	ε_b	0.523	---
mean particle diameter	d_p	1.27	mm
effective thermal conductivity in stagnant fluid	k_{eo}	0.11034	W/m K
effective thermal conductivity adjacent to wall in stagnant fluid	k_{ewo}	0.0576	W/m K
heat capacity	C_b, C_w	1.486	kJ/kg K

Experimental adsorption isotherms determined by Quirit (2000) for Amelco® silica gel beads were used to determine the coefficient and power of the modified Dubinin-Astakov relation. Regression analysis gave the values of w_{sat} and n_F as 0.5248 g water/g silica gel and 0.9265 respectively. All other parameters such as the heat of adsorption, bed heat capacities, densities were estimated from literature values applying appropriate mixing rules and correction factors where needed.

.

Similar to the treatment of Q_u, where significant temperature dependencies are expected, simpler regression equations for parameters or coefficients were obtained. Quirit (2000) shows the derivation of the expression for the isosteric heat of adsorption ΔH_{ads} in terms of temperature, the adsorption potential A, and the Antoine's equation constants b and c (Equation 20).

$$\Delta H_{ads} = -A - \frac{RbT^2}{(T+c)^2} \quad (20)$$

where R is the gas constant. The adsorption potential, defined as the free energy difference between the adsorbed phase and the saturated liquid is given by $A = -RT \ln\left(\frac{P}{P_v}\right)$.

For water, the Antoine's equation constants a, b and c are 16.262, 3799.89 and 226.35 respectively (Smith, et al, 2001).

ΔH_{ads} is evaluated at various values of relative humidity and plotted against uptake w. The isosteric heat of adsorption is found to decrease in magnitude, approaching the heat of vaporization of water as the uptake increases. A fourth-order equation in w is obtained with a goodness of fit or R-squared value of 0.9991.

The regression equation for ΔH_{ads} is substituted into the expression for the coefficient of the dimensionless heat generation. Q'_v was rigorously evaluated at various values of temperature between 25 and 100°C using Equations 12 and 20; and a second-order polynomial was fitted to these results (Equations 21a and 21b) with a goodness of fit or R-squared value of 0.9995.

$$Q'_v = -0.1261T^2 + 73.769T - 10834 \quad (21a)$$

$$Q'_v = -1363.8\phi^2 + 205.01\phi - 79.429 \quad (21b)$$

3. NUMERICAL SOLUTION

The computational domain is chosen to be the section of the adsorption panel, taking advantage of symmetry about a rod fin. A rod fin in the mid-section of the bed is selected so as not to have to account for edge effects. The domain is divided into discrete rectangular volume elements, each of width Δx, length Δy and height Δz except in and around the fin domain, where the volume elements are cylindrical shells of thickness Δr and height Δz. The sizes of Δx, Δy, Δr and Δz are not uniform throughout the domain with finer grids about metal-adsorbent interfaces. The three-dimensional grid comprising our computational domain is shown in Figure 3 and Figure 4.

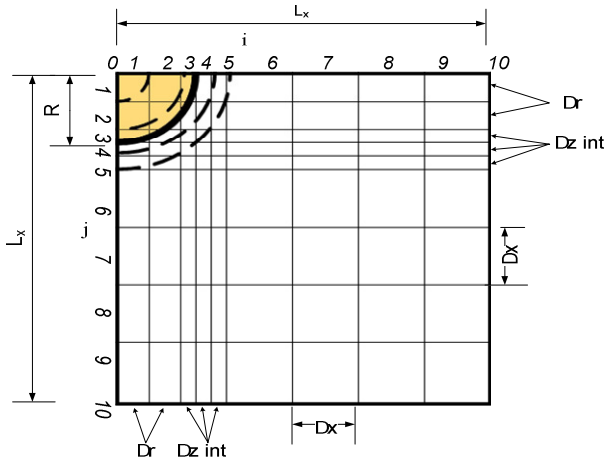

Figure 3: Grid generation on the computational domain about a rod fin (top view)

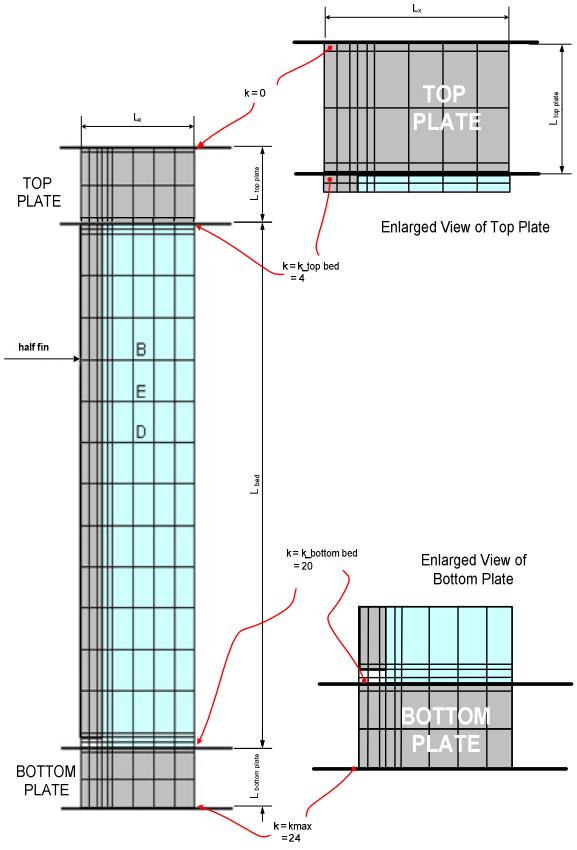

Figure 4: Grid generation on the computational domain (side view) with total height $L_{top\ plate} + L_{bed} + L_{bottom\ plate}$ and widths L_x measured from the center of a rod fin

The smallest thickness of volume element in the three-dimensional grid comprising the computational domain is based on the assumption that the thermal conductivity of the bed next to the metal wall is uniform over the thickness of half the average particle diameter (Ofuchi and Kunii, 1965). With an average particle diameter of 1.27 mm, the thickness of this volume element is 0.635 mm. The volume element on the metal wall next to this bed is assigned the same size so that the thermal conductivity between these two volume elements can be conveniently given by the geometric mean of their thermal conductivities as suggested by Patankar (1980).

The length and time scales used in the numerical solution were checked against the criteria for continuum treatment given by Kaviany (1991) and the criteria for local thermal equilibrium derived by Carbonell and Whitaker (1984) and validated by Glatzmaier and Ramirez (1988).

The dimensionless heat equation is solved using the method of lines to yield temperature progressions and profiles that may be compared with experimental temperature progressions and profiles to evaluate effective thermal conductivities and apparent diffusivities in the bed.

The effective thermal conductivity correction factor f_k is defined as the ratio of the apparent thermal conductivity observed from experimental data k_b to that in stagnant fluid predicted by the Kunii-Smith correlation $k_{eo.}$ The correction factor is evaluated by fitting the model to measured temperature profiles in the bed during heating and cooling.

The heat generation correction factor, defined as the ratio of the Dubinin-Astakhov equilibrium heat generation q_{veq} over the apparent or observed heat generation q_v, is evaluated by fitting the model to measured temperature progressions of the bed during desorption and adsorption.

The dimensionless energy equation given by Equation 14 was solved using the Method of Lines (MOL). Application of the MOL discretizes all derivatives with respect to all independent variables except time, resulting in a system of first order ordinary differential equations (ODE's) which is then solved using initial value methods.

For the purpose of quickly determining trends, the Euler method was used for the earlier runs. Thereafter, the second order Runge-Kutta method was used in order to have a second order accuracy.

Furthermore, the explicit solution was used for easier programming and to ensure convergence provided the time increment used was adequately small. The time increment used was found by trial and error, guided initially by the criteria for the validity of continuum treatment and local thermal equilibrium assumption. Once a time increment that gave a convergence was found, additional runs were done using smaller time increments to ensure that the first successful convergence was not a mere accidental convergence. The same runs were used to determine the extent of error propagation per time iteration. A dimensionless time increment $\Delta\tau = 0.00052$ was used in most of the simulation runs.

For simulating the heating and cooling sequence, the initialization step involved generating the 3-dimensional matrices of (1) dimensionless temperatures ϕ, (2) the uptake w, and (3) the heat generation Q_v. Every element in each matrix corresponds to each volume element in the computational domain. Initial values were assigned corresponding to a uniform temperature equal to a room temperature of 303 K. The reservoir temperature was also assigned a constant value of $T_{res} = 299$ K, the average value from experimental runs.

After initialization, the iterations were started. The top boundary condition was imposed and calculations were carried out for all grid points (k, j, i). The coefficients of the energy equation were evaluated for each volume element during the first iteration in the heating mode and again during the first iteration of the cooling mode. These were stored in memory for succeeding iterations.

For the second order Runge-Kutta method, the term $\partial\phi/\partial\tau$ for each grid point was evaluated twice in each time iteration. Both evaluations were used in the estimation of the new set of dimensionless temperature ϕ_{kji} for the new time step. The boundary conditions were then applied and the uptake matrix updated using the new set of temperatures. The heat generation term matrix was updated during the evaluation of $\partial\phi/\partial\tau$.

The program code was written in C++ and runs were done for two different values of I_{tot}, 559 and 745 W/m^2, corresponding to the experimental average radiant intensity from the lamps at different intensity settings.

4. RESULTS AND DISCUSSION

Numerous simulation runs were performed using various values of the correction factors for the effective thermal conductivity f_k and for the heat generation f_{qv} to find the values that will give good agreement between simulation outputs and time-smoothed experimental data at two different levels of radiant heat intensity. Parametric studies were done to indicate the effect of f_k and f_{qv} on temperature profile and progressions.

4.1 Significance of the effective thermal conductivity correction factor f_k

It was observed from parametric studies that f_k influenced the temperature profile as indicated by the difference between the top plate and bed temperatures. As f_k increases, the bed and plate temperatures approach each other. Increasing values of f_k improve heat transfer and increasingly limits the top plate temperature.

The effective thermal conductivity correction factor f_k is defined as the ratio of the apparent effective thermal conductivity k_{app} observed from experimental data to the effective thermal conductivity in stagnant fluid predicted by the Kunii-Smith correlation k_{eo}. The higher value of k_{app}, here approximately 9 to 15 times larger than k_{eo} implies from $k_b = k_{eo} + k_{ef}$ that the effective thermal conductivity of the bed must include a contribution from fluid currents arising from the temperature differences between the metal walls and the adsorbent bed, as well as a contribution from mass transfer effects.

4.2 Significance of the heat generation correction factor f_{qv}

The heat generation factor f_{qv} is defined as the ratio of the equilibrium heat generation over the apparent heat generation. Its value corresponds to how closely the system approaches phase equilibrium. This approach to phase equilibrium conditions can be limited by mass transfer rates. Slower desorption and adsorption rates result in slow approach to equilibrium conditions and are indicated by large values of f_{qv}. The relationship between the heat generation factor fqc and the observed rate of uptake dw'/dt can be shown to be

Parametric studies show that during heating accompanied by desorption, the rate of temperature rise of the bed increases as f_{qv} increases. Likewise during cooling accompanied by adsorption, the rate of temperature drop of the bed increases as f_{qv} increases. The temperatures reached by the bed when f_{qv} is infinite correspond to the temperatures of a non-adsorbing system, or one whose heat of adsorption is zero. Such a condition may be reached when the bed is saturated.

For the model output to match the February 27 experimental data run at I_{tot} = 559 W/m^2, the rate of heat generation must be lower than the equilibrium rate of heat generation by a factor 1/f_{qv}, where f_{qv} was found to have a value of 27 during heating and 35 during cooling. For the March 1 experimental data run at I_{tot} = 745 W/m^2, f_{qv} value at lower bed temperatures was 35 and at higher bed temperatures, 70. This trend is unlike that for the February 27 run. The higher f_{qv} at higher temperatures for the March 1 run is indicative of much lower amounts desorbed at these temperatures. This can be explained by the faster rate of desorption in the earlier part of the run resulting in the earlier depletion of adsorbed specie.

The relationship between the heat generation factor f_{qv} and the observed rate of uptake dw'/dt can be derived. Observed rates of uptake can be calculated from the best fit values of f_{qv}.

Figure 5 and Figure 6 show the progression of calculated observed rates of uptake at different values of f_{qv} that match experimental data. Comparing the two figures for the same f_{qv}, the observed rates of uptake are larger for I_{tot} = 745 W/m^2, which is associated with faster rates of temperature change during heating.

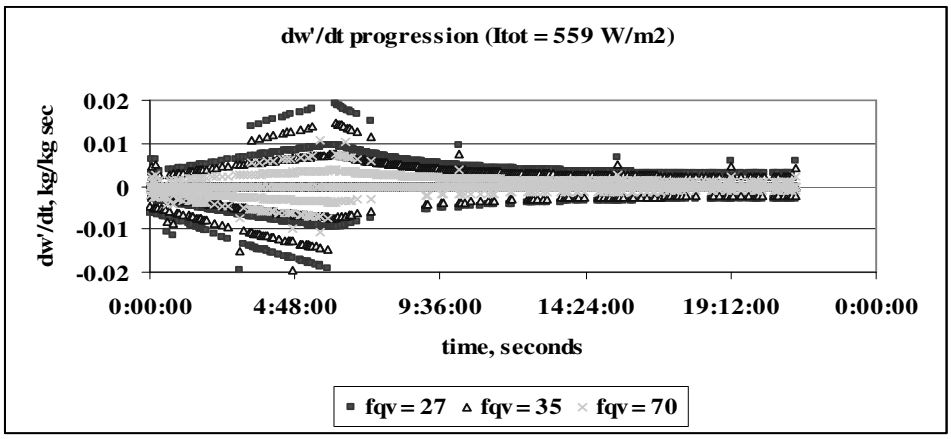

Figure 1: Rate of observed uptake for different values of f_{qv} (I_{tot} = 559W/m2)

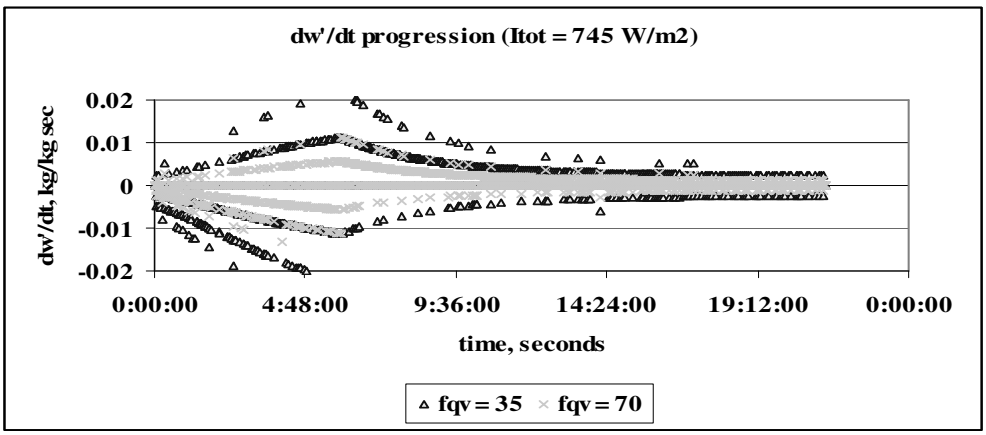

Figure 2: Rate of observed uptake for different values of f_{qv} (I_{tot} = 745 W/m2)

Figure 7 compares the calculated observed rates of uptake with rates of uptake when $f_{qv} = 1$ for $I_{tot} = 559$ W/m^2. The latter corresponds to rates of uptake if equilibrium were assumed at all times. Observed rates of uptake are smaller than equilibrium uptake rates by at least one order of magnitude.

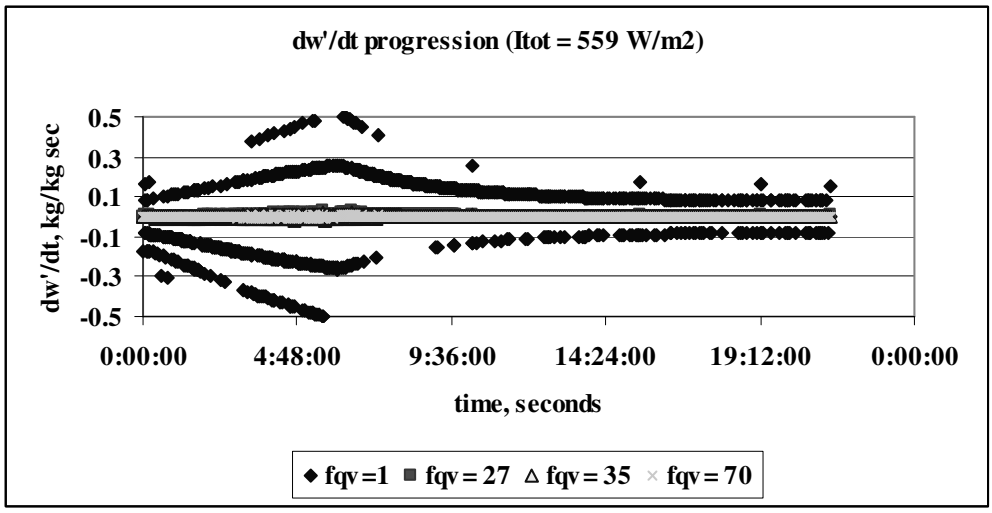

Figure 3: Comparison of rates of observed uptake with equilibrium rates of uptake ($f_{qv} = 1$)

If we assume surface diffusion to be controlling, we are able to estimate the effective surface diffusivity D_s from observed uptake rates. Table 2 shows mean values of the effective surface diffusivities for different f_{qv} calculated from measured temperature progressions on experiment runs using $I_{tot} = 559$ W/m^2 and 745 W/m^2. The values range from 1.05 x 10^{-10} to 8.89 x 10^{-10} m^2/s, which are within the range of values measured by Ni and San (2002) and those suggested by the pre-exponential factor and activation energy determined by Chihara and Suzuki (1983).

Table 2 Effective surface diffusivity Ds calculated from measured temperature progressions.

	Effective surface diffusivity, D_s(m^2/s)					
	$I_{tot} = 559$ W/m^2			$I_{tot} = 745$ W/m^2		
	fqv = 27	*fqv = 35*	*fqv = 70*	*fqv = 27*	*fqv = 35*	*fqv = 70*
mean D_s	8.89E-10	8.84E-10	8.79E-10	1.05E-10	1.06E-10	1.073E-10
maximum D_s	2.85E-07	2.85E-07	2.85E-07	5.61E-09	5.68E-09	6.015E-09
minimum D_s	1.96E-11	1.97E-11	1.98E-11	1.55E-11	1.55E-11	1.56E-11

4.3 Heat and Mass Transfer Rates from Temperature Profiles and Progressive

The rate of heat generation is higher for the equilibrium model than that observed. There is a difference between the observed heat generation during adsorption at low bed temperatures and that observed during desorption at high bed temperatures. At I_{tot} = 559 W/m^2, the rate of equilibrium heat generation is higher than the observed rate of heat generation by a factor of 27 to 35 during desorption, and by a factor of 35 during adsorption. Interestingly, the observation is reversed for I_{tot} = 745 W/m^2 wherein the factor is 70 during desorption and 35 during adsorption.

The heat generation correction factor is a measure of the system's approach to rates that give equilibrium uptakes at the prevailing bed temperature and pressure. The approach to equilibrium is limited by mass transfer, whereby the faster the rate of mass transfer, the faster will be the approach to equilibrium.

5. CONCLUSIONS AND RECOMMENDATIONS

This work expressed the 3D equation of energy in terms of only temperature as the dependent variable with correction factors for the assumptions of static bed conduction and equilibrium uptakes. Using the simulation, performing regression analysis and comparing the simulation runs with experiment, this work was able to plot apparent the apparent rate of uptake with time and evaluate an apparent thermal conductivity of a packed bed of silica gel and an apparent mass diffusivity for the bed.

ACKNOWLEDGEMENT

The authors wish to acknowledge the support of the Department of Science and Technology and the World Bank Engineering and Science Education Project (DOST-WB ESEP) for the PhD Fellowship grant, the UP Engineering Research and Development Foundation, the UP Chemical Engineering Alumni Foundation for supplementary funding, Dr. Henry Ramos of the National Institute of Physics for advice and assistance, and the University of the Philippines, Diliman Chancellor for the PhD Incentive Grant through the Office of the Vice Chancellor for Research and Development.

REFERENCES

1. Aittomaki, A. and A. Aula (1991), "Determination of Effective Thermal conductivity of Adsorbant Bed Using Measured Temperature Profiles," *Int. Comm. Heat Mass Transfer,* v. 18, pp. 681-690.
2. Batchelor G.K. and R.W. O'Brien (1977), "Thermal and Electrical Conduction through a Granular Material," *Proc. Roy. Soc. (London),* A355, pp.313-333.
3. Brodkey, R.S. and H.C. Hershey (1988), Transport Phenomena: a unified approach, McGraw-Hill, New York.
4. Carbonell, R.G. and Whitaker, S., (1984), "Heat and Mass transfer in Porous Media," in *Fundamentals of Transport Phenomena in Porous Media,* Bear and Corapcioglu, eds., Martinus Nijhoff Publishers., 121-198.
5. Chihara K. and M. Suzuki (1983), *J. Chem Eng. Japan* v. 16, 293.

6. Cortes, F.B., F. Chejne, J.M. Mejia and C.A. Londono (2009), "Mathematical model of the sorption phenomenon of methanol in activated coal," *Energy Conversion and Management,* v. 50, no.5 , pp. 1295-1303.
7. Cutlip, M.B. and M. Shacham (1998), "The Numerical Method of Lines for Partial Differential Equations," *CACHE News*, p. 18.
8. Douglas, J. and J.E. Gunn (1964), "A General Formulation of Alternating Direction Implicit Methods, Part I, Parabolic and Hyperbolic Problems," *Numerische Mathematik*, v.4, pp. 41-63.
9. Fedorov A. and R. Viskanta (1999), "Analysis of Transient Heat/Mass Transfer and Adsorption/Desorption Interactions," *International Journal of Heat and Mass Transfer*, v. 42, no. 5, pp. 803-820.
10. Garg, H.P. and J. Prakash, (2000), Solar Energy Fundamentals and Application, 1st revised ed, Tata McGraw-Hill Publishing Company Limited, New Delhi.
11. Glatzmaier, G.C. and Ramirez, W.F., 1988, "Use of Volume Averaging for the Modeling of thermal Properties of Porous Materials," *Chem. Eng., Sci.*, v.43, pp.3157-3169.
12. Guilleminot, J.J., F. Meunier and J. Pakleza (1987), "Heat and Mass Transfer in a Non-isothermal Fixed Bed Solid Asorbent Reactor : A Uniform Pressure Non-uniform Temperature Case", *International Journal of Heat Mass Transfer*, v. 30, no. 8, pp. 1595-1606.
13. Gurgel, J.M. (1998), "Thermal Conductivity of silica gel/water," *High Temperatures - High Pressures,* v. 30, no.3, pp. 315-320.
14. Gurgel, J. M, L.S. Andrade Filho, Ph. Grenier and F.Meunier (2001), "Thermal Diffusivity and Adsorption Kinetics of Silica Gel/Water", *Adsorption,* v. 7, no.3, pp.211-219.
15. Hajji and Khalloufi (1995), Theoretical and Experimental investigation of a Constant-Pressure Adsorption Process", International Journal of Heat and Mass Transfer, v. 38, no. 18, pp. 3349-3358.
16. Hassan, H.J., AA. Mohamad, and R. Bennacer (2011), "Simulation of an adsorption solar cooling system », *Energy*, v. 36, Issue 1, pp. 530-537.
17. Kaviany, M (1991), Principles of Heat Transfer in Porous Media, Springer-Verlag New York Inc., New York, NY.
18. Klein, S.A., (1975), "Calculation of Flat-Plate Loss Coefficients," Solar Energy, v.17, 79.
19. Kremer, D. (1994), "Method of Lines for the Analysis of Optical Waveguide Structures with Complex Refractive Indices using a Pole-Free Eigenvalue Determination", *Electron. Lett.,* v. 30, no. 13, pp. 1088-1090.
20. Kunii, D. and J.M. Smith (1960), Heat transfer characteristics of porous rocks. AIChE J., v. 6 no.1, pp. 71-78.
21. Leong K.C. and Y. Liu (2004), "Numerical Study of a Combined Heat and Mass Recovery Adsorption Cooling Cycle," *International Journal of Heat and Mass Transfer*, v. 47, pp. 4761-4770.
22. Marletta, L. G. Maggio, A. Freni, M. Ingrasciotta, and G. Restuccia (2002), 'A non-uniform Temprature non-Uniform Pressure Dynamic Model of Heat and Mass Transfer in Compact Adsorbent Beds,' *International Journal of Heat and Mass Transfer* v. 45, pp. 3321-3330.
23. Ni, C.C. and J.Y. San (2002), "Measurement of Apparent Solid-Side Mass Diffusivity of a Water Vapor-Silica Gel System," *International Journal of Heat and Mass Transfer*, v. 45, pp.1839-1847.
24. Ofuchi, K. and D. Kunii (1965), Heat Transfer characteristics of packed beds with stagnant fluids, Int. J. Heat Mass. Transfer, v. 8, pp. 749-757.

25. Passos, E.F. J. F. Escobedo and F. Meunier (1989), "Simulation of an intermittent adsorptive solar cooling system, Solar Energy, v.42, no. 2, pp.103-111.
26. Patankar, S.V. (1980), Numerical Heat Transfer and Fluid Flow, Hemisphere Publishing Corp.
27. Peaceman, D.W. and H.H. Rachford (1955), "The Numerical Solution of Parabolic and Elliptic Differential Equations", *Journal Soc. Ind. Appl. Math*, v. 3, p.28.
28. Pons, M. (1998), "Full Analysis of Internal Adsorbate Redistribution in Regenerative Adsorprtion Cycles," *Adsorption,* 4, pp. 299-311.
29. Qin, W. and H. Baoqui (2001), "Determination and Analysis of the Effective Diffusivity of Adsorption Refrigeration Working Pair", *ACTA Energiae Solaris Sinica*, v. 22.
30. Quirit, L.L., E.S. Ramos and P.C. Pabroa (2000), "Study of Adsorption of Water Vapor on Silica Gel", Natural Sciences Research Institute Technical Report.
31. Sakoda, A. and Suzuki, M. (1986), "Simultaneous transport of heat and adsorbate in closed type adsorption cooling system using solar heat." *Journal of Solar Engineering*, v. 108, p. 239.
32. Scheisser, W. E. (1991), *The Numerical Method of Lines Integration of Partial Differential Equations,* Academic Press, San Diego
33. Smith, J. M., H.C. VanNess and M.M. Abbott (2001), Introduction to Chemical Engineering Thermodynamics, 6th edition, McGraw-Hill, Singapore.
34. Sun et al (1986), "Calculation of Temperature and concentration distributions inside a spherical solid adsorbent grain submitted to a pressure step of adsorbable vapor," *Int. J. Heat and Mass Transfer* v.29 no.9, pp.1393-1406.
35. Suzuki, M and K. Kawazoe (1974), *J. Chem. Eng. Japan,* v.7, 346.
36. Suzuki, M. and K. Kawazoe (1975), *J. Chem Eng. Japan,* v.8.
37. Suzuki, M., (1989), Adsorption Engineering, Elsevier Science Publishers B.V.
38. Yang, W.D. and R. Pregla (1995), "The Method of Lines for Analysis of Waveguide Structure with Multidiscontinuities", *Electron. Lett.*, v. 31, no. 11, pp. 892-893.
39. Yaws, C.L. (2009), Transport Properties of Chemicals and Hydrocarbons: Viscosity, Thermal Conductivity and Diffusivity of C1 toC100 Organics and Ar to Zr inorganics, William Andrew Publishing.
40. Yong, L. and K. Sumathy (2004), "Comparison Between Heat Transfer and Heat Mass Transfer Models for Transportation Process in an Adsorbent Bed," *International Journal of Heat and Mass Transfer*, v. 47, pp. 1587-1598.
41. Zhang, G., D.D. Wang, J.P. Zhang, Y.P. Han, and Wanchao Sun (2011), "Simulation of operating characteristics of the silica gel-water adsorption chiller powered by solar energy", *Solar Energy,* v. 85, Issue 7, pp. 1469-1478.

